TWENTY-FIFTH EUROPEAN ROTORCRAFT FORUM

Paper n° C4

INTERACTIONAL AERODYNAMICS OF HELICOPTER CONFIGURATIONS. APPLICATION OF A BEM METHODOLOGY

BY

A. VISINGARDI, A. D'ALASCIO
CIRA, ITALY

SEPTEMBER 14-16, 1999
ROME
ITALY

ASSOCIAZIONE INDUSTRIE PER L'AEROSPAZIO, I SISTEMI E LA DIFESA
ASSOCIAZIONE ITALIANA DI AERONAUTICA ED ASTRONAUTICA

INTERACTIONAL AERODYNAMICS OF HELICOPTER CONFIGURATIONS. APPLICATION OF A BEM METHODOLOGY

A. Visingardi, A. D'Alascio
CIRA, Italian Aerospace Research Center
Capua, Italy

Abstract

The CIRA unsteady panel code RAMSYS (**R**otorcraft **A**erodynamic Modelling **SYS**tem) is applied to the interactional aerodynamic analysis of rotor/fuselage configurations. The original free-wake model and the interactional technique, which have proved their ability to accurately model weak to mild interactional aspects, are further improved in order to analyse the more severe conditions of close body/wake interactions. The wake stability is augmented by the application of a progressive stiffening technique and a wake smoothing. The interactional technique is improved in the selection of the wake panels to cancel. The validation of the code is performed on the AGARD-AR303 test data relative to the University of Maryland rotor/fuselage configuration. A comparison with the experiment is made in terms of wake displacement and time history of the pressure distribution at five transducers located in the plane of symmetry of the configuration on the top of the body surface. The time-averaged pressure distribution along the top part and left side of the fuselage are also shown. The work represents a first attempt of the authors at modelling this kind of problem and useful indications for further developments are obtained by the analysis of the results obtained.

List of Symbols

B, C, F	body source, doublet and wake doublet influence coefficient
c	blade chord
C_p	unsteady pressure coefficient perturbation about the time-averaged value, C_p^m, normalized by $\rho\Omega^2R^2/100$
C_p^m	time-averaged unsteady pressure coefficient normalized by $\rho\Omega^2R^2/100$
C_T/σ	thrust coefficient
L	fuselage length
R	rotor radius
t	time
X	coordinate along fuselage axis
$\mathbf{x}$	position vector
$\mathbf{x}_*$	control point position vector
μ	advance ratio
Ω	rotor angular velocity
ϕ	velocity potential
ψ	normalwash/blade azimuthal position
ρ	density
ϱ	distance $\parallel \mathbf{x} - \mathbf{x}_* \parallel$
σ	rotor solidity
$\Delta\phi$	velocity potential jump

1. Introduction

Helicopters operate in a highly complex flowfield which is three-dimensional and unsteady, dominated by the strong vortices of the rotor wake. The close proximity of the various helicopter components and the wake emanating from them give rise to serious interactional problems characterized by unsteadiness in the flow ranging from low to high frequencies. The rotor blades may interact with their associated tip vortices (Blade Vortex Interaction, BVI) thus determining a typical noise known as Blade Slap. The functionality of the tail rotor as well as the empennage can be strongly altered by the interaction with the main rotor wake thus sensibly reducing their efficacy. Considering the role of the fuselage, its displacement effect distorts the onset flow resulting in a non-uniform angle of attack distribution in the rotor disk. The rotor wake is deformed due to the presence of the fuselage which in turn alters the unsteady interaction process between rotor blades and their wake. The

occurrence and the intensity of these interactional effects basically depend on three main factors: flight regime, blade loading and clearence between the rotor and the airframe. In this sense, hover and low-speed forward flight are particularly severe flight regimes during which the vortical system of the wake exerts the strongest interaction with the airframe. Higher blade loadings and/or smaller rotor-airframe clearence contribute to intensify the interactional problem.

The complexity of the interactional phenomenology is such that its experimental and theoretical investigation has represented a real challenge to the helicopter aerodynamics research community for several years. Nowadays, despite many interactional aerodynamic phenomena have been identified [1], the details are still very difficult to model because the physics of these flowfields involve a complex balance of pressure, inertial, and viscous effects. The work of Sheridan and co-workers [1] represents the first systematic investigation of the problem. This work has analysed the problem associated with rotor/body and rotor/empennage interactions tracing useful general design guidelines to the minimization of the problem. Several experimental works [1, 2, 3, 4] have highlighted the induction of significant mean pressure loads by the rotor wake on the fuselage. Further works [1, 5, 6] have then also shown that the unsteady pressure fluctuation determine a substantial form of loading over many parts of the fuselage. A valuable, systematic experimental investigation of the interactional problem has been commenced more recently by Leishman, Crouse, Bi *et al.* who have carried out a series of tests on a simplified but representative fuselage body with a four-bladed rotor in different flight conditions [7]-[9], clarifying, in particular, the nature of body pressure signatures that are due to blade passage effects, close wake interactions, and wake impingement on the body.

One of the earliest theoretical studies of the interactional problem is attributed to Bramwell [10] who employed conformal mapping techniques for predicting interactional effects. Since then a variety of theoretical approaches have been proposed by researchers and an exhaustive illustration of these methodologies can be found in [11]. If Euler/Navier-Stokes based methodologies are in theory able to take inherently into account of the interactional effects, they still today suffer from serious limitations which hamper their application so that the methodologies based on the potential equations still represent the most viable tools for the analysis of the interactional problem. Landgrebe, Moffitt and Clark [12, 13] employed a panel code to compute the upwash determined by the fuselage on the rotor disk in order to adjust the inflow angles to the rotor in the trim analysis. Conversely, Freeman [14] applied Hess panel code to represent the fuselage of a helicopter and included a time-averaged vortex tube wake model during the calculation of the body aerodynamics. Mavris *et al.* [15] coupled Scully's lifting line code to a panelled fuselage without considering the distortion of the wake in presence of the body. Lorber and Egolf [16] were the first to recognise the importance of the wake distortion due to the body and developed a prescribed wake analysis which could take into account of the wake distortion about the body via geometric displacement rules. A more sophisticated method was proposed by Berry [17] who applied a vortex lattice model of the rotor wake able to distort under the influence of the body. Nevertheless, no special treatement of the close interaction between the rotor wake and the body was introduced. More recently, more sophisticated methodologies have been proposed. Quackenbush *et al.* [18] have employed a lifting surface representation of the rotor and a source/doublet representation of the fuselage. A constant vorticity contour (CVC) free wake model has been employed to capture the details of the blade tip vortex. Close body/wake interactions have been accurately represented by the application of an analytical numerical matching (ANM) of the induced velocity field of curved vortex elements in close proximity to the body. The results obtained have shown a very good correlation with the experimental results. A comprehensive model, named MURFI, has also been proposed by Crouse, Leishman, and Bi [9] with which

the interactional problem has been faced by coupling a source panel model of the body, a lifting line approach for the rotor, a prescribed model of the rotor wake and a simplified model of interaction between the body and the wake. The results obtained have indicated a good agreement with the expermental results. Clark and Maskew [19] have proposed a more comprehensive approach to the problem with which the rotor, the fuselage and the wake have been represented by source and doublet singularities. The methodology has provided accurate results for the cases involving the intersection of the wake with the body.

The panel code RAMSYS [20], developed at CIRA, belongs to this last category. The aim of this work is to illustrate the improvements introduced in RAMSYS for the wake modelling and the interactional technique in order to analyse the more severe conditions of close body/wake interactions. The results obtained so far by the application of the code to a rotor/fuselage configuration in forward flight are then compared with the available test results.

2. Description of RAMSYS

RAMSYS is an unsteady panel code for multibody configurations based on Morino's boundary integral formulation.

The formulation consists in the solution of Laplace's equation written in terms of the velocity potential ϕ

$$\nabla^2\phi = 0 \qquad \forall \mathbf{x} \notin \mathcal{S}(t) \qquad (1)$$

such that $\mathbf{v} = \nabla\phi$. $\mathcal{S}(t)$ is a surface outside of which the flow is potential and consists of a surface S_B surrounding the body geometry and a surface S_W surrounding the wake geometry.

The boundary condition at infinity is that $\phi = 0$. The surface of the body is assumed to be impermeable hence $\frac{\partial\phi}{\partial n} = \mathbf{v}_B \cdot \mathbf{n}$ where $\mathbf{v}_B$ is the velocity of a point on the body. The wake is a surface of discontinuity which is not penetrated by the fluid and across which there is no pressure jump. The second wake condition implies that $\Delta\phi$ remains constant following a wake point $\mathbf{x}_W$, and equal to the value it had when $\mathbf{x}_W$ left the trailing edge.

The value of $\Delta\phi$ at the trailing edge is obtained by using the Kutta-Joukowski hypothesis that no vortex filament exists at the trailing edge; this implies that the value of $\Delta\phi$ on the wake and the value of $\Delta\phi$ on the body are equal at the trailing edge.

The application of Green's function method to Eq.(1), yields the following boundary-integral-representation for the velocity potential ϕ

$$E(\mathbf{x}_*)\phi(\mathbf{x}_*, t_*) = I_B + I_W \qquad (2)$$

with

$$I_B = \oiint_S \left[\left(-\frac{1}{4\pi\varrho}\right)\frac{\partial\phi}{\partial n} - \phi\frac{\partial}{\partial n}\left(-\frac{1}{4\pi\varrho}\right)\right] dS$$

and

$$I_W = -\iint_{S_W} \Delta\phi\frac{\partial}{\partial n}\left(-\frac{1}{4\pi\varrho}\right) dS$$

representing respectively the contribution of the body and the wake. $E(\mathbf{x}_*)$ is a domain function defined as zero inside $\mathcal{S}$ and unity elsewhere.

The helicopter geometry and the wake are respectively discretised by M and N hyperboloidal quadrilateral panels on which the unknown velocity potential, the normalwash and the velocity potential jump are constant (zeroth-order formulation). Using the collocation method and setting the collocation points at the centroids of each element on the body geometry, the integral equation, Eq.(2), is replaced by an algebraic linear system of equations for the velocity potential ϕ:

$$E_k\phi_k(t) = \sum_{m=1}^{M} B_{km}\psi_m(t) + \sum_{m=1}^{M} C_{km}\phi_m(t) + \sum_{n=1}^{N} F_{kn}\Delta\phi_m(t) \qquad (3)$$

where B, C, and F are respectively the body source, body doublet, and wake doublet influence

coefficients. A Conjugate Gradient Method (GMRES solver) is applied for the numerical solution of the problem.

A correction of the *classical* Kutta condition [21] is implemented in the code in order to guarantee a zero pressure jump at the trailing edge.

A time-marching free-wake model is implemented in RAMSYS. Wake panels are released at each time step from the trailing edge as the lifting body moves through an inertial frame of reference. Therefore, the shape of the wake is a consequence of the local induced velocities which are evaluated from Eq.(2) as:

$$\begin{aligned} \mathbf{v}_i &= \iint_S \left[\left(-\frac{\varrho}{4\pi\varrho^3}\right)\frac{\partial\phi}{\partial n} - \phi\frac{\partial}{\partial n}\left(-\frac{\varrho}{4\pi\varrho^3}\right)\right] dS \\ &- \iint_{S_W} \Delta\phi \frac{\partial}{\partial n}\left(-\frac{\varrho}{4\pi\varrho^3}\right) dS \end{aligned} \tag{4}$$

A Rankine vortex-core model and the Baron-Boffadossi [22] vortex-core model are available to stabilize the wake.

3. Interactional Technique

The simple use of free-wake modelling can be successfully employed for flight conditions where the interactions between the wake and the rotor are relatively mild. However, for strong interactions in which the wake penetrates the body surface this approach leads to unphysical solutions. The present version of RAMSYS implements the method proposed by Clark and Maskew [23] for body/wake interactions. The method poses its fundamentals on an interpretation of flow visualization data relative to a tip vortex filament approaching and then intersecting a body. As the vortex approaches the body it starts to deform about the body shape and the deformation continues until when the vortex elements which reach the closest proximity to the body disappear in the visualization. What happens to these elements is not very clear, nevertheless the remaining part of the vortex seems to continue to move downward but with a minor local distortion.

The numerical translation of this experience has consisted in simply cancelling the doublet intensities $\Delta\phi$ of those wake panels which penetrate the body but allowing that the same wake panels could regain their intensity if during their motion downward they move outside of the body, which is an implicit assumption of the fact that the vortex filament could reconnect away of the body. The described procedure determines in the wake holes delimited by raw-edges corresponding to vortex segments. If these segments are too close to the body they can induce excessive velocities in the near body panels. For this reason a *safety distance* from the body is then computed with which all the wake panels lying inside it are also cancelled. A user-defined fraction of the maximum side length of the wake panels generated during the first rotor revolution is chosen as safety distance.

The analysis of the numerical results obtained during the interactional technique implementation has highlighted the arising of numerical unphysical oscillations in the pressure coefficient which have turned out to be generated by the finite difference computation of the time derivative of the velocity potential due to the wake $\partial\phi_w/\partial t$. It can be shown that for each wake panel this unsteady term can be written as

$$\frac{\partial\phi_w}{\partial t} = -\mathbf{V}_w \cdot \nabla\phi_w \tag{5}$$

where $\nabla\phi_w$ is the induced velocity induced at a point by the wake panel and $\mathbf{V}_w$ represents the convection velocity of the wake panel.

The pressure coefficient expression therefore results to be expressed as

$$\begin{aligned} C_p &= 100\left(\frac{-2}{\Omega^2 R^2}\right)\left[\frac{\partial\phi_b}{\partial t} + (\mathbf{V}_k - \mathbf{V}_w)\cdot\nabla\phi_w \right. \\ &- \left. \mathbf{V}_k\cdot\nabla\phi + \frac{\nabla\phi\cdot\nabla\phi}{2}\right] \end{aligned} \tag{6}$$

being ϕ_b the velocity potential due to the body, $\phi = \phi_b + \phi_w$ and $\mathbf{V}_k$ the kinematic velocity vector.

4. Wake Smoothing

The numerical analysis of rotor/body interactions by panel methods requires an opportune

coupling between an interactional technique and a proper free-wake modelling. Indeed, if the interactional technique is necessary to avoid non physical overshoots in the solution, a correct free-wake displacement is crucial in evaluating the correct pressure distributions acting on the body.

The application of the pure free-wake model turns out to determine an excessively chaotic vortical system which alters considerably the solution on the body. In order to regularize the wake shape a simple progressive stiffening technique and a smoothing technique have been applied. The progressive stiffening technique consists in evaluating the induced velocities acting on the wake panel nodes as a weighted average between the free-wake induced velocity field and the induced velocity field computed by applying the momentum theory to an isolated rotor. Two cubic polynomials function of the vortex age are used as weighting functions. The smoothing technique is employed in order to avoid the excessive deformation of the wake panels. The technique applied is based on the concept of the elastic membrane. For each wake node i a set of additional velocities are computed according to the expression:

$$\mathbf{Ve}_{ij} = \frac{K}{\Delta t}\mathbf{X}_{ij} \tag{7}$$

being K a user-defined coefficient and $\mathbf{X}_{ij}$ the distance between the i-node and each of the four surrounding j-nodes, Fig. 1. The computed velocities $\mathbf{Ve}$ are such that the net value $\sum_i \sum_j \mathbf{Ve}_{ij} = 0$

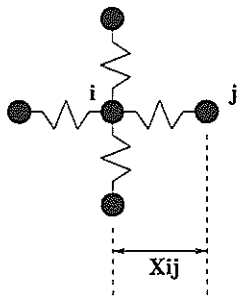

Figure 1: Wake-nodes stencil

5. Test Case for Validation

In order to validate the RAMSYS code on interactional aerodynamic problems the test data published in the AGARD Report AR-303 [24] have been chosen as the reference test cases. These test data refer to the University of Maryland rotor/fuselage configuration. The rotor is a four-bladed fully articulated rotor with $-12°$ linearly twisted rectangular blades with an aspect ratio of 13 and non symmetrical NASA RC(3)10/(4)10 airfoil sections. The fuselage is a simple, analytically defined body of revolution, but however representative of a real helicopter fuselage, generated by a sink and two sources opportunely placed along the x-body axis.

The test case chosen among the available ones is referred to as RUN863. This test case deals with a configuration set at an incidence of $-6°$. Being the rotor shaft axis perpendicular to the body surface the shaft angle is at the same incidence as the fuselage. The advance ratio is equal to $\mu = 0.10$ and the rotor thrust is $C_T/\sigma = 0.091$. The rotor rotation speed is equal to 1860 RPM.

6. Results and Discussion

In order to perform the numerical analysis on the above mentioned configuration the rotor blades have been discretised by 20 panels around the airfoil and 16 panels in the spanwise direction. Not being available the NASA airfoils, the ONERA OA209 airfoil section have been employed for the blades. The fuselage has been discretised by 20 panels in the circumferential direction and 44 panels along the body length. A temporal discretization corresponding to an azimuthal step of $15°$ has been employed for the present test case. Six revolutions of the rotor have been considered and three wake spirals have been employed for the wake modelling. The trim conditions employed, TC1, are those of the experiment and have been kindly provided by Prof. J.G. Leishman of the University of Maryland.

The validation procedure has mainly consisted in evaluating the time history of the pressure distributions at five transducers located in the configuration plane of simmetry along the top side of the body surface, Fig. 2.

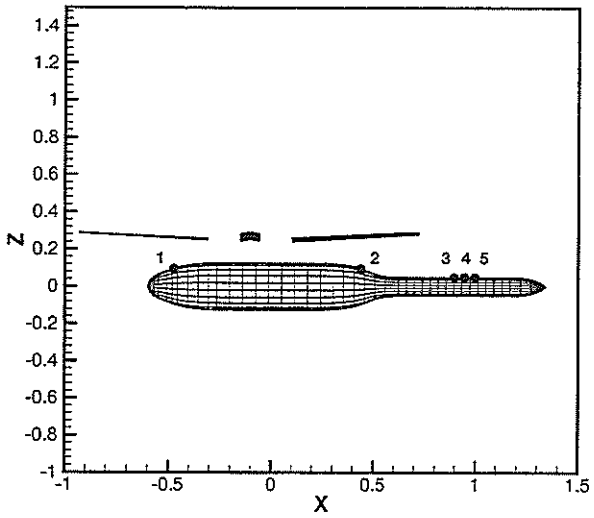

Figure 2: Location of pressure sensors

6.1 Wake Modelling

Figs. 3 and 4 depict the wake displacement about the configuration. Only tip vortices are represented for clarity. The wake, during its convection downward, moves toward the body and starts to distort to conform to the body shape. Approximately just behind the rotor hub an intersection with the body occurs, Fig. 3. How realistic this interaction is, is not very clear.

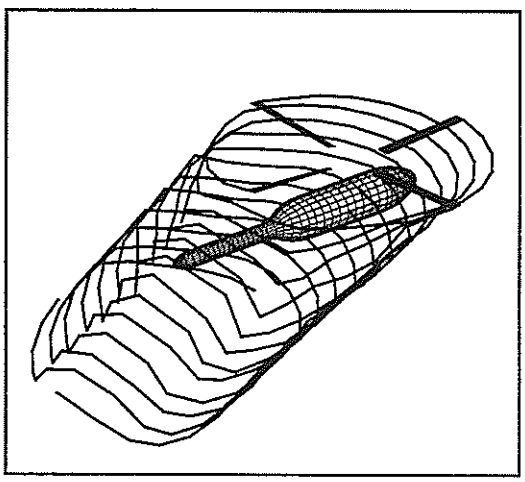

Figure 3: Rotor wake tip vortex geometry

A side view of the wake illustrates very clearly how the tip vortices move downstream following the tail boom surface. Just after the body, the absence of the body reflection makes the wake free to be pushed downward following a different wake skew angle, Fig. 4.

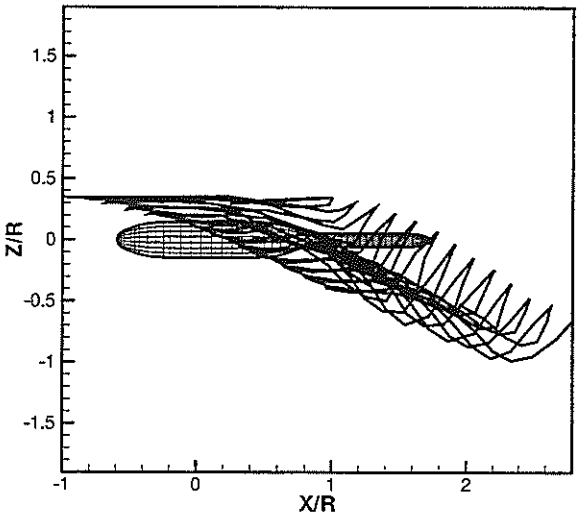

Figure 4: Rotor wake tip vortex geometry. Side view

A crucial point during the numerical modelling of the rotor wake/fuselage interaction problem is the correct displacement of the tip vortices with respect to the body. Fig. 5 illustrates the rotor wake boundary computed by RAMSYS by employing the experimental trim conditions (TC1). It results that the tip vortex moves downstream slowly approaching the rear part of the body but never impacting on it. The tip vortices strongly impact the front part of the body.

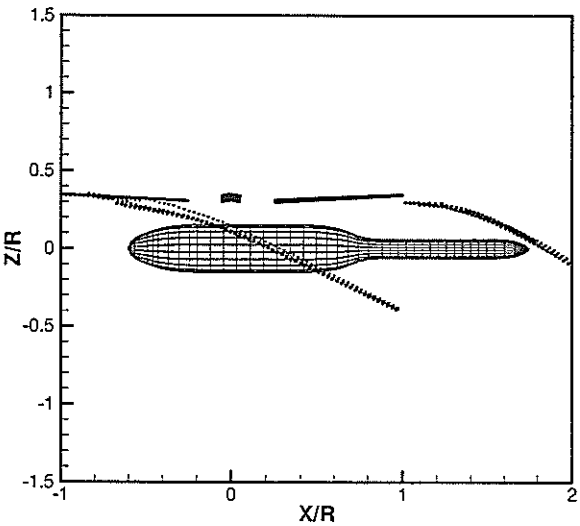

Figure 5: Location of rotor wake boundary. Trim condition 1

The comparison with a flow visualization, even though at a different advance ratio and

presumably different C_T/σ, Fig. 6, illustrates however a very different behaviour. Several numerical investigations consisting in modifying the weighting functions of the progressive stiffening technique have been performed to clarify this point. No substantial changes in the rotor wake boundary have been observed.

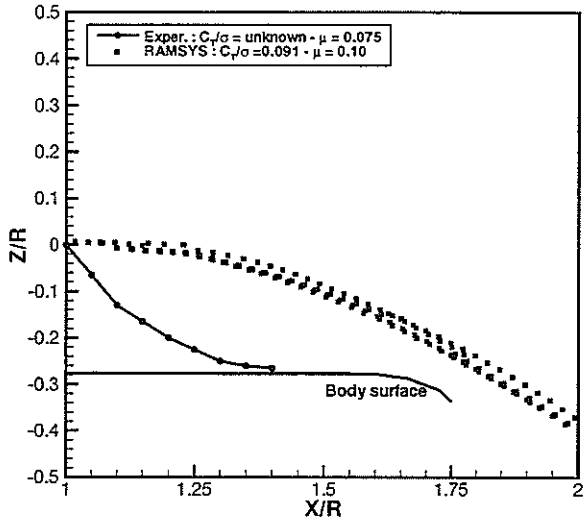

Figure 6: Tip vortex displacement

A second set of trim conditions, TC2, have then been employed in order to verify the influence of the trim conditions on the wake displacement. These trim conditions have been numerically evaluated at Agusta using the ROTOR module in VSAERO [25] and refer to an isolated rotor. The wake displacement obtained by their application, Fig. 7, shows very little changes with respect to that obtained by TC1.

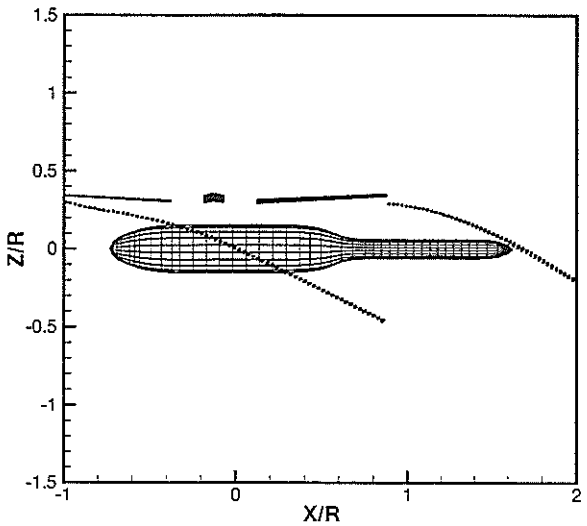

Figure 7: Location of rotor wake boundary. Trim condition 2

6.2 Time History Pressure Distribution

The numerical data employed for the comparison have been taken during the last revolution of the rotor. A filtering has been performed on the unsteady results in order to separate the time averaged pressure values from the pure unsteady part. Furthermore, in analogy with the experimental data elaboration, an ensamble averaging of the numerical results over 90° of the blade azimuth angle has been performed in order to remove some numerical non-periodicities introduced by the free-wake modelling.

6.2.1 Trim Conditions TC1

Fig. 8 illustrates the time history of the pressure distribution evaluated at transducer #1. The agreement between the numerical results and the experiment is very satisfactory. Indeed, at the location of this transducer, the only contribution to the C_p evolution in time is merely due to the blade passage as it can be observed by the pressure peaks occurring in phase with the blade passages on the body [24]. The wake, as also shown in Fig. 5, passes well away from the transducer.

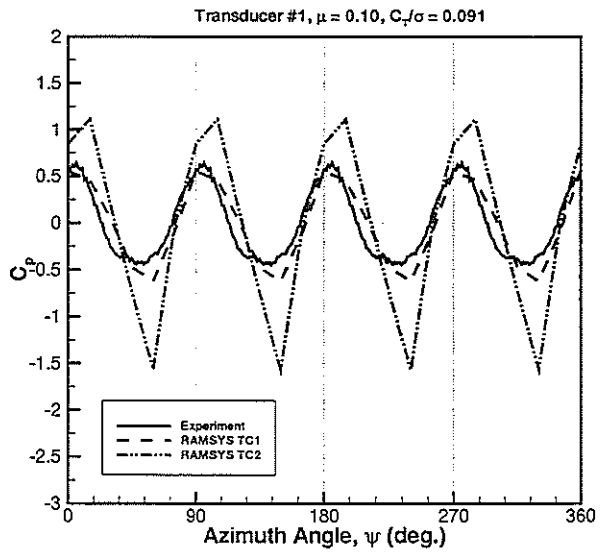

Figure 8: Time history C_p at transducer #1

The behaviour at transducer #2 changes considerably. The transducer is located in a region which is totally immersed in the vortical system

even though the tip vortices don't seem to play a significant role. In this region the numerical wake penetrates the fuselage. The agreement between RAMSYS and the experiment is fair only on the qualitative point of view. The two signals are in phase. As for transducer #1, the C_p evolution in time is only due to the blade passage [24] and this explains the phase agreement between RAMSYS and the experiment. Nevertheless, an excessive overestimation is visible in the numerical results. This behaviour is likely to be due to the passage of the root vortex filament. Indeed, the potential methodology has turned out to evaluate an intensity for this filament which seems to be higher than the correct one. More investigation is required on this problem, Fig. 9.

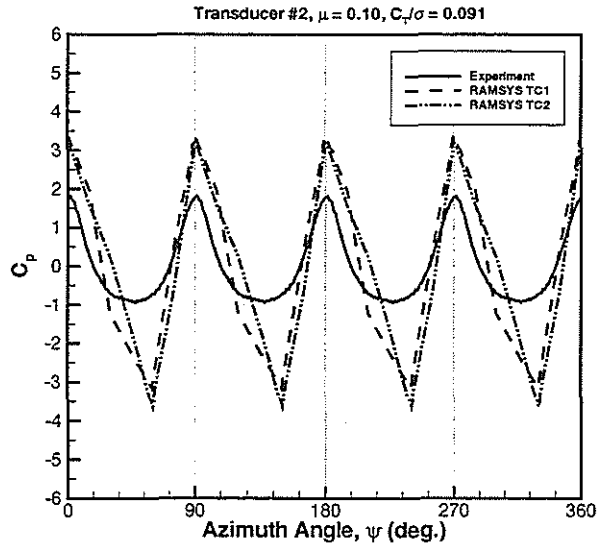

Figure 9: Time history C_p at transducer #2

Fig. 10 shows the unsteady pressures measured at transducer #3. At this location the experimental results denote a tip vortex which is approaching the body surface interaction. The behaviour is similar to that showed at transducer #1 but with a slight phase shift denoting that the body starts to feel the presence of the vortex. The numerical results reflect what has been observed in Fig. 6. The tip vortex is much farther from the body than that observed in the experiment. This explains the smaller fluctuation of the pressure and the in-phase pressure peaks with the blade passage on the body surface. The agreement with the experiment is only qualitative.

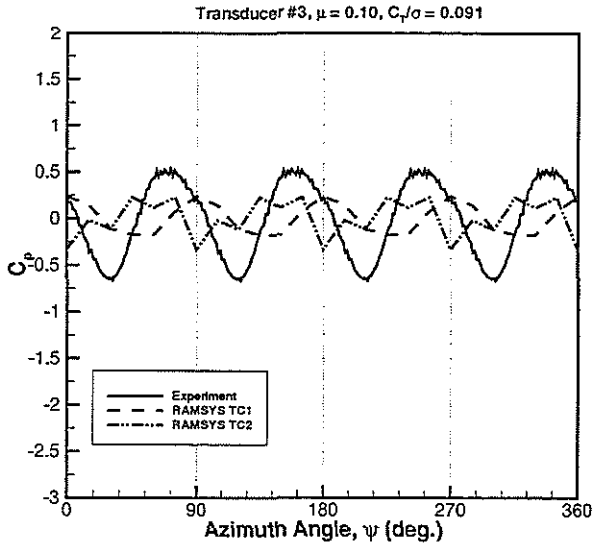

Figure 10: Time history C_p at transducer #3

In Fig. 11 the experimental pressure fluctuation denotes a further vortex approaching to the fuselage. The peaks increase their amplitude. The numerical results don't show a sensitive amplitude increase with respect to those obtained at transducer #3.

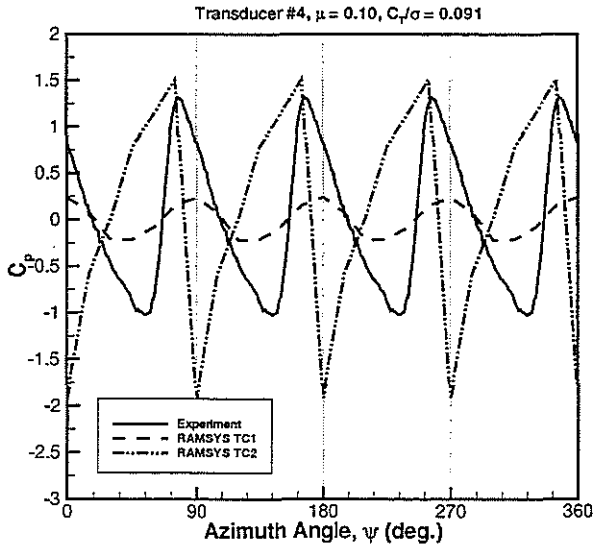

Figure 11: Time history C_p at transducer #4

Fig. 12 illustrates a close vortex/surface interaction. The shape of the experimental and numerical results change considerably and also the amplitudes increase. The numerical result indicates that the fuselage starts to feel the presence of the tip vortex with a considerable delay with respect to the experiment.

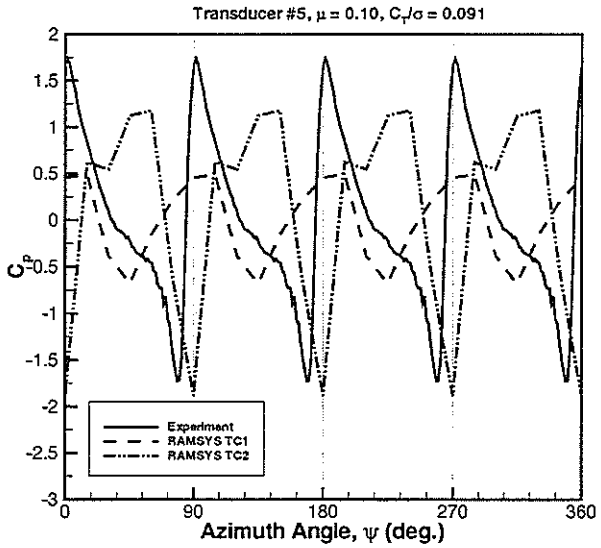

Figure 12: Time history C_p at transducer #5

6.2.2 Trim Conditions TC2

The numerical evaluation of the time history pressure distributions has also been made by applying the trim conditions TC2. Fluctuations higher than the experiment have been predicted at transducer #1, Fig. 8. This behaviour can be easily explained by the closer vicinity of the upstream rotor wake boundary to the transducer (see also Fig. 7). No significant changes are observed at transducer #2, and this could confirm the interpretation for which the main contribution to the pressure fluctuations should be determined by the root vortices passage, Fig. 9. A more irregular pressure signal is obtained at transducer #3. The amplitude remains unchanged but a sort of phase shift, in the same direction as the experiment becomes visible, Fig. 10. The results obtained at transducers #4 and #5 are worth noting only for the considerable amplitude increase, which follows what happens in the experiment, Figs. 11 and 12. Despite only little differences are shown in the wake boundary displacement between TC1 and TC2, an increase in the tip vortex strength is obtained with TC2 which turns out to determine dramatic differences in the pressure signals in terms of amplitude and phase shift.

6.3 Time-averaged Pressure Distribution

A qualitative comparison in terms of the time-averaged pressure distribution along the body top surface is illustrated in Fig. 13. The two results are not comparable due to the different flight conditions. The diagram nevertheless gives interesting information on the numerical modelling. As in the experiment the pressure increases in the region where higher becomes the dynamic pressure below the rotor [8]. According to this behaviour the difference in the value of the pressure peak between the experiment and RAMSYS can be easily explained. Indeed, the experimental advance ratio is lower than the numerical one and so is the thrust coefficient. Consequently, the velocities that originate behind the rotor of the numerical test case are higher, with a resulting increase in the dynamic pressure. Some numerical overshoots have been observed in the last part of the tail boom. The results have not been represented. The considerable difference between the wake panels and the body panels dimensions in this region may possibly generate these instabilities. Nevertheless a further analysis of the problem is necessary.

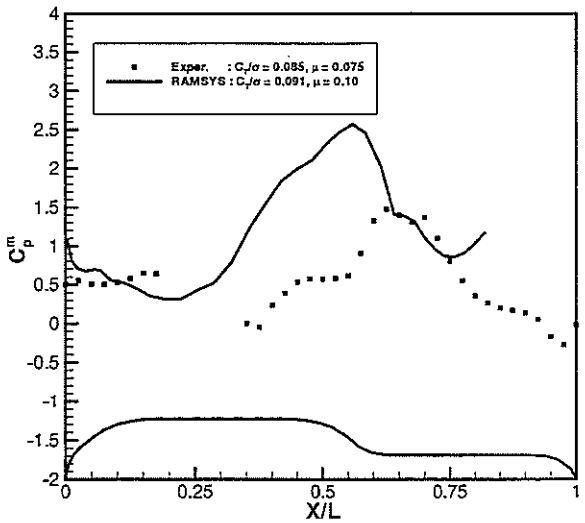

Figure 13: Time-averaged pressure distribution on body top

Fig. 14, finally illustrates a qualitative comparison in terms of the time-averaged pressure distribution along the left side of the fuselage. The high suction peaks visible in both results are due to the strong rotor downwash that is present in that region, reaching their highest value in correspondence of the rotor

disk edge [8]. The qualitative agreement between the two results is in this sense good.

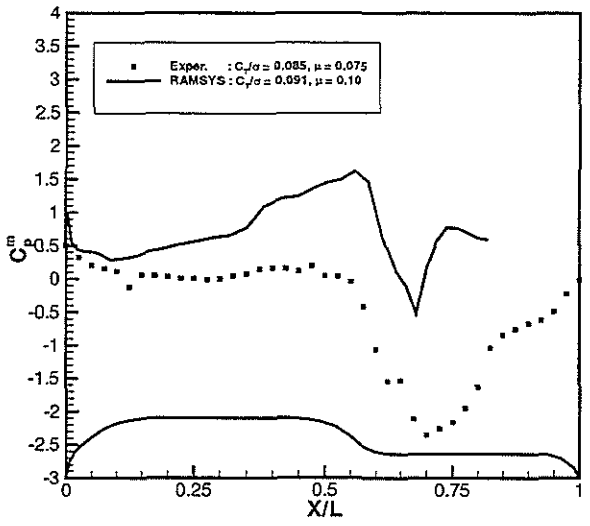

Figure 14: Time-averaged pressure distribution on body left side

7. Conclusions

The results obtained during the present validation indicate that the crucial point in the analysis of aerodynamic interactional problems is the acccurate modelling of the wake. Indeed, the tip vortex displacement and the wake stability play a fundamental role for the correct evaluation of the loads acting on the body. In particular the following conclusions can be made:

- a general, qualitative accordance with the available flow visualization has been observed in terms of the vortex displacement about the body. Nevertheless, the analysis of the rotor wake boundaries has highlighted a different behaviour between RAMSYS and the experiment in terms of the tip vortex trajectory in the tail boom region. The flow visualization indicates a tip vortex approaching the body surface much faster. This occurrence might explain quite satisfactorily the underestimation which the numerical results show in reproducing the time history of the pressure distribution at the transducers located in this region. In order to better evaluate the wake boundaries, several numerical investigations have been made by modifying the wake stiffness. No significant improvements have been obtained.

- The use of different trim conditions, despite evaluated for an isolated rotor, set at the same experimental flight conditions, have determined substantial changes in the pressure signals in the same direction as the experimental results. This behaviour has clearly indicated that the evaluation of the trim conditions constitutes a fundamental aspect to take into account during the interactional aerodynamic analysis of helicopter configurations.

- The time-averaged pressure distribution on the top and the left side of the fuselage show a qualitative agreement with the experimental results.

The present work has represented a first step made by the authors in modelling the interactional aerodynamics of a rotor/fuselage configuration. The experience made so far and the results obtained have provided useful indications for the improvement of the methodology mainly directed to a more satisfactory solution of the free-wake modelling problem and a coupled trim methodology.

8. Acknowledgements

Most of this work was funded by Agusta, a Finmeccanica Company, under contract - N.98/395/FAV. The authors particularly wish to thank Professor Paolo Luchini of the Politecnico di Milano who is collaborating, under contract CIRA Order No. 980472, to the improvement of the methodology, Professor J. Gordon Leishman of the University of Maryland for providing the experimental data and the relative trim conditions and Ing. A. Saporiti of Agusta for providing the numerical trim conditions.

References

[1] P.F. Sheridan, and R.P. Smith, Interactional Aerodynamics - A New Challenge to Helicopter Technology, American Helicopter Society 35th Annual Forum, Washington, D.C., May 1979.

[2] J.C. Wilson, and R.E. Mineck, Wind-Tunnel Investigation of Helicopter Rotor Wake Effects on Three Helicopter Fuselage Models, NASA TM X-3185, 1975.

[3] C.A. Smith, and M.D. Betzina, Aerodynamic Loads Induced by a Rotor on a Body of Revolution, Journal of the American Helicopter Society, Vol. 31, (1), Jan. 1986.

[4] H.M. McMahon, N.M. Komerath, and J.E. Hubbard, Studies of Rotor-Airframe Interactions in Forward Flight, AIAA Paper 85-5015, AIAA 3rd Applied Aerodynamics Conference, Colorado Springs, Col., Oct. 1985.

[5] N.M. Komerath, H.M. McMahon, and J.E. Hubbard, Aerodynamic Interactions between a Rotor and Airframe in Forward Flight, AIAA Paper 85-1606, AIAA 18th Fluid Dynamics, Plasma Dynamics and Lasers Conference, Cincinnati, Ohio, Jul. 1985.

[6] S.G. Liu, N.M. Komerath, and H.M. McMahon, Velocity Measurements of Airframe Effects on a Rotor in Low-Speed Forward Flight, AIAA Journal of Aircraft, Vol. 26, (4), Apr. 1984.

[7] A. Bagai, and J.G. Leishman, Experimental Study of Rotor Wake/Body Interactions in Hover, Journal of the American Helicopter Society, Vol. 37, (4), Oct. 1992.

[8] J.G. Leishman, and Nai-Pei Bi, Aerodynamic Interactions Between a Rotor and a Fuselage in Forward Flight, American Helicopter Society, 45th Annual Forum, Boston, Mass., May 1989.

[9] G.L. Crouse Jr., J.G. Leishman, and Nai-Pei Bi, Theoretical and Experimental Study of Unsteady Rotor/Body Aerodynamic Interactions, Journal of the American Helicopter Society, Vol. 37, (1), Jan. 1992.

[10] A. Bramwell, A Theory of the Aerodynamic Interference Between a Helicopter Rotor Blade and a Fuselage and Wing in Hovering and Forward Flight, Journal of Sound and Vibration, Vol.3, (3), 1966.

[11] B.D. Charles, and A.A. Hassan, Airframe Interference Effects On Rotorcraft BVI, American Helicopter Society, 55th, Annual Forum, Montreal, Canada, May 1999.

[12] A.J., Landgrebe, R.C., Moffitt, and D.R. Clark, Aerodynamic Technology for Advanced Rotorcraft - Part I", Journal of the American Helicopter Society, Vol.22, (2), Apr. 1977.

[13] A.J., Landgrebe, R.C., Moffitt, and D.R. Clark, Aerodynamic Technology for Advanced Rotorcraft - Part I", Journal of the American Helicopter Society, Vol.22, (3), Jul. 1977.

[14] C.E. Freeman, Development and Validation of a Combined Rotor-Fuselage Induced Flow-Field Computational Method, NASA Technical Paper 1656, Jun. 1980.

[15] D.N. Mavris, N.M. Komerath, and H.M. McMahon, Prediction of Aerodynamic Rotor-Airframe Interactions in Forward Flight", Journal of the American Helicopter Society, Vol. 34, N.4, Oct. 1989.

[16] P.F. Lorber, and T.A. Egolf, An Unsteady Helicopter Rotor-Fuselage Aerodynamic Interaction, Journal of the American Helicopter Society, Vol. 35, N.3, Jul. 1990.

[17] J.D. Berry, Prediction of Time-Dependent Fuselage Pressures in the Wake of a Helicopter Rotor, 2nd International Conference on Rotorcraft Basic Research, University of Maryland, College Park, MD, Feb. 1988.

[18] T.R., Quackenbush, C-MG. Lam, and D.B. Bliss, Vortex Methods for the Computational Analysis of Rotor/Body Interaction", Journal of the American Helicopter Society, Vol. 39, N.4, Oct. 1994.

[19] D.R. Clark, and B. Maskew, A Re-Examination of the Aerodynamics of Hovering Rotors Including the Presence of the Fuselage, International Technical Specialists' Meeting on Rotorcraft Basic Research, Atlanta, Georgia, Mar. 1991.

[20] A. Visingardi, A. D'Alascio, A. Pagano, and P. Renzoni, Validation of CIRA's Rotorcraft Aerodynamic Modelling SYStem with DNW experimental Data, 22th European Rotorcraft Forum, Brighton, UK, 1996.

[21] A. D'Alascio, A. Visingardi, and P. Renzoni, Explicit Kutta Condition Correction for Rotary Wing Flows, 19th World Conference on the Boundary Element Method, Rome, Italy, Sep. 1997

[22] A. Baron, and M. Boffadossi, Numerical Simulation of Unsteady Rotor Wakes, 17th European Rotorcraft Forum, Berlin, Germany, Sep. 1991.

[23] D.R. Clark, and B. Maskew, Calculation of Unsteady Rotor Blade Loads and Blade/Fuselage Interference, II International Conference on Rotorcraft Basic Research, College Park, U.S.A., Feb. 1988.

[24] J.G., Leishman, and Nai-Pei Bi, Experimental Data on the Aerodynamic Interactions Between a Helicopter Rotor and an Airframe, published in: A Selection of Experimental Test Cases for the Validation of CFD Codes, AGARD-AR-303, Aug 1994.

[25] AMI Inc., VSAERO - A Computer Program for Calculating the Nonlinear Aerodynamic Characteristics of Arbitrary Configurations, Version 6.0 Users' Manual, Nov. 1997.